Nuclear Engineering and Technology 56 (2024) 2610–2624

Contents lists available at ScienceDirect

Nuclear Engineering and Technology

journal homepage: www.elsevier.com/locate/net

Original Article

Operating condition optimization of liquid metal heat pipe using deep learning based genetic algorithm: Heat transfer performance

Ik Jae Jin, Dong Hun Lee, In Cheol Bang *

Department of Nuclear Engineering Ulsan National Institute of Science and Technology (UNIST) 50 UNIST-gil, Ulju-gun, Ulsan, 44919, Republic of Korea

ARTICLE INFO

Keywords:
Liquid metal heat pipe
Deep learning
Genetic algorithm
Operating condition optimization
Generalization performance

ABSTRACT

Liquid metal heat pipes play a critical role in various high-temperature applications, with their optimization being pivotal to achieving optimal thermal performance. In this study, a deep learning based genetic algorithm is suggested to optimize the operating conditions of liquid metal heat pipes. The optimization performance was investigated in both single and multi-variable optimization schemes, considering the operating conditions of heat load, inclination angle, and filling ratio. The single-variable optimization indicated reasonable performance for various conditions, reinforcing the potential applicability of the optimization method across a broad spectrum of high-temperature industries. The multi-variable optimization revealed an almost congruent performance level to single-variable optimization, suggesting that the robustness of optimization method is not compromised with additional variables. Furthermore, the generalization performance of the optimization method was investigated by conducting an experimental investigation, proving a similar performance. This study underlines the potential of optimizing the operating condition of heat pipes, with significant consequences in sectors such as high temperature field, thereby offering a pathway to more efficient, cost-effective thermal solutions.

1. Introduction

The heat pipe, a device proficient in transferring heat efficiently, uses two-phase processes, which include evaporation and condensation. This results in low thermal resistance and minimal temperature differences between the heat source and the heat sink. Relying on gravity and capillary force for operation, it doesn't need electricity. The enhanced heat transfer performance of the heat pipe is achieved, benefiting particularly from the capillary force, with development in wick technology. The heat pipe is both easy to maintain and passive, making it an ideal heat removal device for various applications, including electric devices [1], solar power plants [2], and nuclear power plants [3]. In the field of nuclear energy, there's an increasing interest in heat pipes. They have multiple roles such as the removal of heat from spent nuclear fuel and as passive safety systems during accidents [4–7]. A new concept, heat pipe-cooled microreactors, has been introduced recently. Heat pipes facilitate heat removal in these systems. Various heat pipe-cooled microreactors designs aim for high-temperature operations to maximize heat efficiency in electricity generation [8–14]. A liquid metal heat pipe, which possesses high thermal conductivity and low vapor pressure, is the chosen working fluid in the nuclear field. Therefore, heat pipes with liquid metal as the working fluid offer effective heat control, contributing to the stable and efficient operation of heat pipe-cooled microreactor systems. Given that safety is the top priority in nuclear power plants, accurate prediction and optimization of heat pipe performance are essential.

In various industries, heat pipes predominantly employ water as the working fluid. However, when sodium or potassium was utilized as the working fluid of the heat pipe, the thermal properties are less understood, making it difficult to predict heat transfer performance without experimental tests. Therefore, numerous studies have been conducted into the performance of heat pipes that use liquid metals such as sodium and potassium [15–17]. One study explored how thermosiphon performance with sodium as the working fluid was influenced by factors such as filling ratio, which includes dry-out and wall overheating scenarios. It was found that the filling ratio significantly impacts liquid metal thermosiphon heat transfer [18]. Another study offered experimental insights into designing heat pipes that use potassium as the working fluid, focusing on the effects of inclination angle and input power on startup performance. Both inclination and input power were key determinants in assessing heat transfer [19]. For heat pipes operating at high temperatures, empirical studies were conducted to assess the thermal characteristics when potassium served as the working fluid [20]. In

* Corresponding author.
E-mail address: icbang@unist.ac.kr (I.C. Bang).

https://doi.org/10.1016/j.net.2024.02.020
Received 25 September 2023; Received in revised form 10 December 2023; Accepted 10 February 2024
Available online 15 February 2024

Nomenclature

D	diameter [m]
L	axial Length [m]
$\dot{m}$	mass flow rate [kg/s]
C_p	heat capacity [J/K]
h	heat transfer coefficient [W/m^2-K]
T	temperature [°C]
Q	power [W]
P	pressure [Pa]
I	current [A]
V	voltage [V]
ρ	density [kg/m^3]
ε	porosity
x	input
w	weight
y_i	predicted value
$\widehat{y}_i$	reference value

Subscript

sat	saturation
rad	radiation
conv	convection
e	evaporation
a	adiabatic
c	condenser
s	solid
v	vapor
w	wick
o	pipe outer diameter

addition, it was found that inclination angle was a key variable affecting thermal performance, whereas filling ratio had minimal impact [21]. An investigation into the startup and operational condition of heat pipes using sodium was carried out, particularly emphasizing the influence of the inclination angle [22]. Additional studies investigated the heat transfer attributes of heat pipes with different wick structures, using sodium as the working fluid [23]. Due to limited research on the thermal characteristics of liquid metals compared to water, it is challenging to predict the performance of liquid metal heat pipes. Various factors, including two-phase processes such as evaporation and condensation, make this more complex. Furthermore, the wick structure facilitating capillary force adds another layer of complexity. As a result, empirical validation is essential before liquid metal heat pipes can be widely applied across industries. Manufacturing these heat pipes for all possible scenarios incurs substantial costs due to the need to verify their heat transfer capabilities under each unique condition.

Estimating the thermal resistance in heat pipes and thermosiphons is a method that can employ a variety of approaches, from thermal resistance circuit calculations based on theoretical models to numerical analysis involving governing equations [24–29]. These methods, however, often depend on sparse experimental evidence or are valid only within certain operational conditions. These data points usually require experimental observation or assumptions from the saturation temperature related to internal pressure. Traditional models often make specific assumptions and have built-in limitations, which means they may not be able to fully understand or represent the complexity and variety of the system. Because of this, their accuracy and usefulness could be limited, especially when applied to a wide range of situations such as filling ratio. Therefore, creating predictive frameworks for heat pipes that take into account intricate mechanisms of heat and mass transfer is a difficult undertaking.

There's a widespread need for a flexible approach to predicting heat transfer performance across various industries, one that considers the distinctions between thermosiphons and heat pipes. Therefore, the application of machine learning and deep learning methodologies has been suggested to resolve these prediction challenges. Because heat pipe systems can display nonlinear associations among different factors, deep learning is well-suited to model these nonlinear correlations and yield accurate forecasts by learning from data patterns. This capability makes it possible to understand how heat pipes behave under varying conditions and enhances predictive accuracy. Unlike traditional numerical models, deep learning models can also be updated more flexibly to adapt to new data. Therefore, several studies have been conducted on heat pipes using machine learning or deep learning.

The utilization of machine learning and deep learning has been suggested to reduce the difficulty in predicting the heat transfer performance of heat pipes [30,31]. Because the prediction of the thermal performance of a pulsating heat pipe is difficult, artificial neural networks (ANNs) and regression/correlation analysis (RCA)-based thermal performance prediction methods have been suggested [32]. The thermal performance prediction of an ANN model is superior to that of an RCA-based prediction model when geometrical parameters are considered. A method for optimizing the number of fines and filling ratio was proposed using a genetic algorithm [33], and the ANN architecture was used to predict the thermal performance when a genetic algorithm was applied. In another study, a method for predicting the heat transfer performance of a closed vertical pulsating heat pipe was suggested based on the ANN architecture [34]. Based on the results, the ANN architecture predicted the thermal performance of the closed vertical pulsating heat pipe with a maximum percentage error of 20% in the data range. Additionally, researchers compared the ANN, deep neural network (DNN), and convolutional neural network (CNN) architectures to predict the outlet temperature of the condenser for a heat pipe [35]. The overall prediction performance of the CNN architecture was superior to those of the ANN and DNN architectures. However, the DNN architecture indicated a lower maximum percentage error than the CNN architecture. Heat transfer performance prediction studies, which numerically analyze behavior, have been mainly proposed based on thermosiphons because of the complexity of the capillary force. In addition, previous studies considered only a few input parameters to predict the thermal performance of heat pipes. In other words, the heat transfer performance prediction method was applied under limited conditions, such as the same heat pipe and operating conditions. Such limitations could result in the deep learning models being overfitted to the training data, compromising their ability to generalize to new conditions. Given the risk of overfitting, it's crucial to assess performance in settings where the data varies, either geometrically or in terms of operational conditions. To demonstrate the method's adaptability, evaluation should extend beyond the range of the training dataset. Furthermore, adjusting the model architecture could enhance its predictive performance. Alongside the prediction model, optimization methods should also be taken into account to suggest the optimal condition.

This study suggests a method that combines deep learning and genetic algorithms for optimizing the operational conditions to enhance the thermal performance of heat pipes that use liquid metal as a working fluid. The heat transfer performance of a heat pipe is linked to its thermal resistance. To ensure optimal performance, an accurate prediction model is essential, which is why deep learning techniques are employed in this study. Data for both training and test were obtained from published literatures that experimentally investigated the performance of heat pipes with liquid metal as the working fluid. The generalization performance of the optimization model was conducted using experimental data, which was carried out in this paper. Predictions

about thermal performance are based on a variety of factors, including operating conditions, the properties of the liquid metal, and geometrical information of the wick. This study proposes to deviate from using operational boundary conditions in heat pipes, in contrast to empirical correlation or governing equation methods. The study introduces a method for predicting and optimizing heat transfer performance without experimental data. Optimizing the thermal performance of heat pipes that use liquid metal can potentially improve both cost-efficiency and safety in industries that operate at high temperatures.

2. Modeling and methodology

2.1. Configation of dataset

In this research, the dataset employed for training and assessing the prediction performance for heat pipes using liquid metal as a working fluid was obtained from published articles. Liquid metals, specifically pure sodium and pure potassium, which are actively researched in the nuclear field, were considered as the working fluids for the heat pipes in the deep learning-based thermal performance prediction method. In this study, wickless heat pipes (thermosiphon) and screen mesh heat pipes were considered. The data relating to the operating condition of heat pipes were included, considering start-up and steady-state data. Thermal resistance in these heat pipes is influenced by numerous variables, given their operation based on two-phase processes. Therefore, an extensive set of variables was considered in the deep learning training. These variables include heat load, inclination angle, filling ratio, inner and outer diameters, and lengths corresponding to various sections of the heat pipe (evaporation, adiabatic, and condensation), along with the thermal properties of the wick structure and working fluids involved. When calculating the filling ratio for Thermosiphon, the filling ratio is determined through the ratio of the volume in the evaporation section. However, when calculating the filling ratio for the screen mesh heat pipe, the filling ratio is determined through the ratio of the entire wick's volume. Therefore, the filling ratio is denoted in 'g' units to avoid confusion. While assuming the adiabatic section's temperature as the saturation temperature improves prediction performance under specific boundary conditions, these variables remain unknown without dedicated experiments. The study introduces a method for predicting and optimizing heat transfer performance without experimental data. The objective is to predict liquid metal heat pipe performance solely based on initial properties, considering thermal properties that encompass information about initial conditions, which are determined by pressure. Based on each article, the range of each parameter used for deep learning applications is summarized in Table 1 [19–23]. Despite the wide range of variables considered, one challenge encountered was the limited availability of experimental studies focusing on liquid metal heat pipes using either sodium or potassium. Consequently, the dataset was not enough for deep learning model training. In situations where the dataset for training a deep learning model is scarce, data augmentation techniques can be employed to overcome this limitation. Recently, interpolation has been introduced as an effective data augmentation strategy, especially for time-series and text data, with the aim of performance improvement [36–38]. In the context of this study, multiple published articles offer thermal resistance values in relation to heat load. This gives valuable insights into how thermal resistance varies with changes in heat load. This information was crucial for applying data augmentation via interpolation, treating the thermal resistance as a function of heat load similar to a time-series dataset. Therefore, data augmentation techniques, specifically interpolation methods, were applied to enhance the model's performance. The augmented data enhanced the prediction performance of the deep learning model. Of the total 29,014 datasets, 80% was allocated for training and validation, with the remaining 20% used for testing.

Table 1
Range of each parameter obtained from published literature.

Parameter	Range
Heat load (W)	20–4135
Thermal resistance (K/W)	0.01043–2.4997
Inclination angle (°)	0–90
Filling ratio (g)	8–100
Inner diameter (mm)	20–30
Outer diameter (mm)	16–23
Le/L (%)	28.571–40
La/L (%)	14.286–25
Lc/L (%)	40–57.143
L (mm)	350–1000
Thermal conductivity (W/cm°C)	16.3
Liquid metal density (kg/m^3)	664–740
Liquid metal thermal conductivity (W/cm°C)	0.307–0.486
Viscosity (centipoise)	0.13–0.149
Specific heat (J/g°C)	0.783–1.549
Wick porosity	1.0–0.634
Wick thickness (mm)	0–5

Data normalization holds specific benefits when it is used for training deep learning models. It helps to mitigate issues such as vanishing or exploding gradients, thereby enhancing model stability. In this study, Z-score normalization was employed for the input data and thermal resistance. This technique transforms the data into a standard normal distribution, having a mean of zero and a standard deviation of one. The approach is relatively immune to outliers and provides consistent outcomes irrespective of the initial data distribution. The equation for Z-score normalization used in this study is given as Equation (1), where $y_{i,norm}$ is normalized data, y_i is data, m is the mean, and σ is the standard deviation.

$$y_{i,norm} = \frac{y_i - m}{\sigma} \tag{1}$$

2.2. Configuration of deep learning model

2.2.1. ANN and DNN

ANNs are computational frameworks modeled from the human brain's biological neural network [39]. ANNs consist of nodes, known as artificial neurons, that process information and forward it to subsequent nodes. The architecture of an ANN typically includes three categories of layers: input, hidden, and output. The network's performance is notably influenced by the number of nodes and the hidden layers. Each node in the hidden layer computes its output based on a set of weights and biases. The output of any given neuron is a nonlinear function applied to the sum of its input signals. The formula that represents the output of a node in the hidden layer, considering both weight and bias, can be seen in Equation (2), where x_i and y_i stand for the input and output, w_{ij} represents the weight.

$$y_i = f\left(\sum\left(x_i \times w_{ij} + bias\right)\right) \tag{2}$$

In recent times, ANNs have enhanced regression capabilities across various applications. When an ANN includes multiple hidden layers, it is categorized as a DNN. In this study, the performance of both ANN and DNN architectures was assessed to identify the optimal thermal performance prediction model for heat pipes using liquid metal as the working fluid. The architectures of both ANN and DNN were optimized by varying the number of nodes [30]. An increase in the number of nodes corresponded to improvement in prediction accuracy. For this study on thermal performance prediction of liquid metal heat pipes, the ANN architecture had 512 nodes in the hidden layer. The DNN variant included three hidden layers, each containing 512 nodes. Representations of the ANN and DNN architectures are shown in Fig. 1.

2.2.2. CNN

Within the realm of deep learning, CNNs have exhibited exceptional capabilities for managing complex data sets, especially in the field of

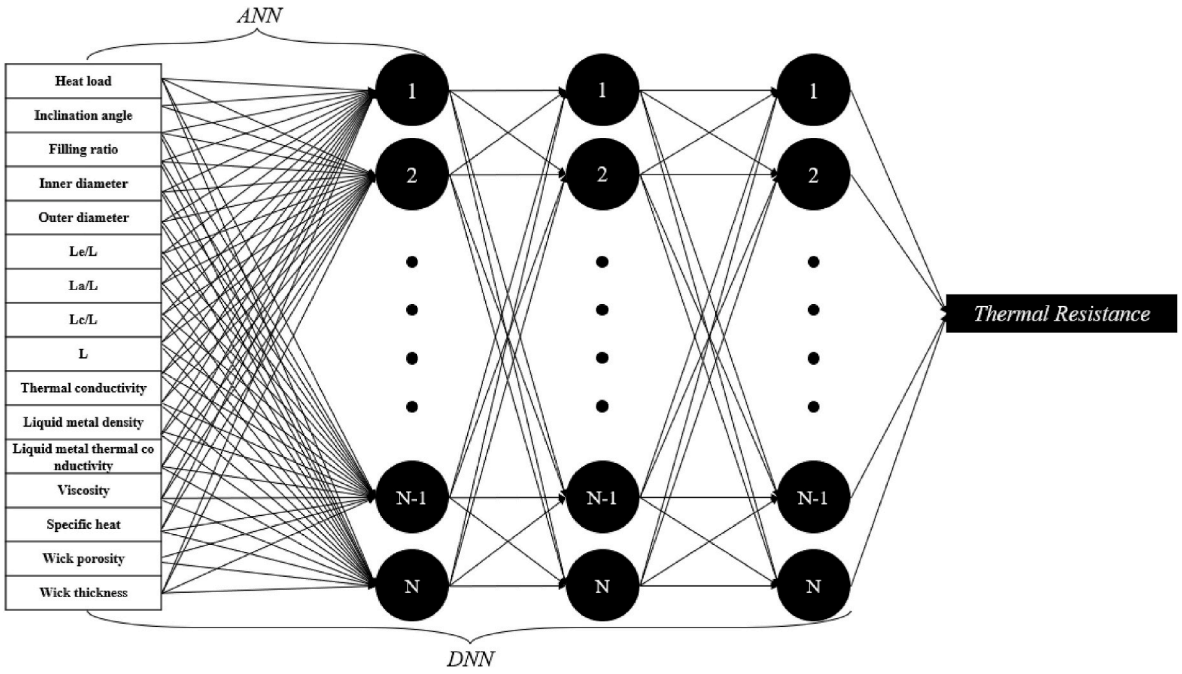

Fig. 1. Architectures of ANN and DNN used for this study [31].

image analysis [40]. CNNs are a specialized type of ANN that generally demand fewer parameters for data manipulation than their traditional ANN. Given these strengths, this study adopted a CNN-based architecture to predict the heat transfer performance of liquid metal heat pipes. While CNNs are predominantly deployed for intricate image data handling, their architecture can be modified to accommodate input parameters specific to heat transfer performance prediction. These parameters often present more extensive data than previous investigations, which consider heat pipe. However, the number of parameters is still lower compared to the image data. The CNNs used in this study were built using one-dimensional convolutional layers, making them simpler than those typically used for image analysis. One of the challenges with deep learning architectures is that increasing the depth beyond an optimal point can result in the loss of important data features, thus degrading the performance. To mitigate this, a skip connection technique was implemented in CNN architecture. This approach preserves essential data features by directly forwarding them from earlier layers to subsequent convolutional layers. In this study, both the standard CNN and the CNN with skip connections were examined to identify the most effective deep-learning architecture for predicting heat transfer performance in liquid metal heat pipes [30]. These two CNN architectures, including the skip connection represented by a blue line, are represented in Fig. 2.

In deep learning architectures, the selection of an activation function is crucial as it dictates how the processed data is activated or deactivated across layers, subsequently influencing the final output. In this study, the Rectified Linear Unit (ReLU) served as the activation function across all considered architectures: ANNs, DNNs, and CNNs. The ReLU function can be formally described by Equation (3), where x is input.

$$ReLU(x) = \begin{cases} ReLU(x) = x, x \geq 0 \\ ReLU(x) = 0, x < 0 \end{cases} \quad (3)$$

Various activation functions like Sigmoid, Tanh, and ReLU exist, but ReLU stands out for its ability to mitigate the vanishing gradient

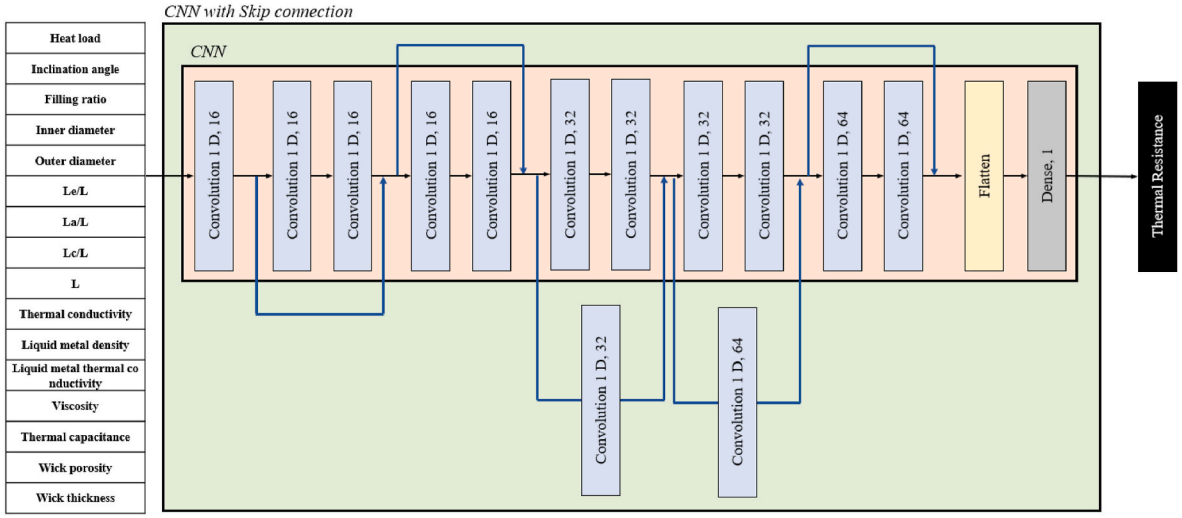

Fig. 2. The architectures of CNN and CNN applied to the skip connection used for this study [31].

problem and facilitate prompt learning. The limitation of ReLU is its output of zero for all negative input values. However, given that our dataset consists exclusively of positive thermal resistance values, this drawback is effectively neutralized, enabling the unrestricted use of ReLU in this study condition. For the training of all architectures, a batch size of 64 was employed. The optimization was carried out using the Adaptive Momentum Estimation (Adam) algorithm, set at a learning rate of 0.001. Adam offers multiple advantages, such as automatic learning rate adjustment and the incorporation of prior gradient information through momentum, thus accelerating convergence while enhancing accuracy. This study utilized the Adam optimizer, largely due to its demonstrable superiority over alternative optimization techniques. K-fold cross-validation was applied to prevent overfitting and enhance the performance of deep learning architecture, where k was set to 5. For comparing the optimal performance of each architecture, the model with the lowest validation loss during 1000 training iterations was used to evaluate prediction performance. Therefore, the epoch at best performance is the number of iterations at the lowest validation loss during 1000 training iterations. Table 2 represents the training conditions and the number of parameters for each of the architectures, identifying the best-performing model for heat pipe heat transfer prediction. The number of parameters represents the total count of trainable weights in the neural network, quantifying the model's capacity and complexity. The reason why the number of parameters varies between architectures, it that it reflects their distinctive features and computational complexities.

2.2.3. Performance evaluation of deep learning architectures

Evaluating the performance of a regression model is fundamentally related to the concept of a loss function. This function calculates the discrepancy between the predicted values and reference values. Adjustments to weights and biases in the deep learning architecture are made to minimize the error, as dictated by the loss function. For this reason, the performance assessment was conducted using a range of commonly employed loss functions [30]. In this study, various metrics were considered for evaluating the performance of the deep learning regression model. These include Percentage Error (PE), Mean Absolute Percentage Error (MAPE), Mean Absolute Error (MAE), Mean Square Error (MSE), and the Coefficient of Determination. (R^2) were considered to evaluate the heat transfer prediction performance of the heat pipe using several performance evaluation methods. Equation (4) through (8) define each of these performance assessment metrics. In these equations, y_i stands for the reference value, $\hat{y}_i$ is the predicted output, $\bar{y}$ denotes the mean of the output values, and n represents the total number of data points in the sample. By adopting these performance metrics, this study offers a comprehensive evaluation of the regression model's accuracy and reliability in predicting heat pipe heat transfer performance.

$$Percentage\ Error\ (PE) = \frac{|\hat{y}_i - y_i|}{y_i} \tag{4}$$

$$Mean\ Absolute\ Percentage\ Error\ (MAPE) = \frac{\sum_{i=1}^{n} \frac{|\hat{y}_i - y_i|}{y_i}}{n} \tag{5}$$

$$Mean\ Absolute\ Error\ (MAE) = \frac{\sum_{i=1}^{n} |y_i - \hat{y}_i|}{n} \tag{6}$$

$$Mean\ Square\ Error\ (MSE) = \frac{\sum_{i=1}^{n} (y_i - \hat{y}_i)^2}{n} \tag{7}$$

$$Coefficient\ of\ determination\ \left(R^2\right) = 1 - \frac{\sum_{i=1}^{n} |y_i - \hat{y}_i|}{\sum_{i=1}^{n} |y_i - \bar{y}|} \tag{8}$$

The prediction performance of a deep learning model is influenced not only by the architecture but also by the selection of the loss function. To identify the optimal training conditions, various loss functions such as MAE, MSE, and MAPE were evaluated for their impact on predictive performance. Although the overall performance was similar within 10%, the loss function, which exhibited the lowest maximum Percentage Error (PE) in prediction, was MSE. The model trained with MSE had a maximum PE of 1.36%, whereas the model trained with MAE had a maximum PE of 2.81%, and the model trained with MAPE had a maximum PE of 1.73%. Therefore, the MSE was used as loss function. Most loss functions involve calculating the difference between predicted and reference values, leading to higher maximum percentage errors, particularly in regions of low thermal resistance. To mitigate this, the models were retrained using normalized values for reference thermal resistance of the liquid metal heat pipe. This adjustment improved the prediction accuracy of the deep learning models, confirming the importance of tailored loss function selection for optimized training outcomes.

2.2.4. Explainable deep learning

The need for clear understanding in deep learning becomes crucial for explaining the complexities of deep learning architecture, clarifying how features contribute, and improving overall model understanding. Therefore, explainable deep learning is essential for transparency, as it assesses the impact of individual features. The interpretation of deep learning based regression models was conducted. Although there are various ways in which the analysis can be performed, SHAP (Shapley Additive exPlanations) was considered [41]. SHAP makes the deep learning model interpretable, rooted in cooperative game theory and Shapley values, fairly distributing the contribution of each variable to interpret model predictions. SHAP provides a detailed understanding of how each variable influences model outcomes in the interpretation of deep learning architecture. Furthermore, SHAP is suitable for analyzing complex models such as CNNs, offering insights into variable importance. The analytical framework employed by SHAP involves the utilization of equation (9) to systematically examine the impact of variables used in predictions: where $\varphi_i(f)$: Shapley value for feature i in the function f, representing the contribution of feature i to the prediction, N: set of all feature values, S: subset of feature values excluding feature i, $f(S\cup\{i\})$: prediction of the model when both feature i and the subset S are present, and $f(S)$: prediction of model when only the subset S is represent.

$$\varphi_i(f) = \sum_{S\in N\setminus\{i\}} \frac{|S|!(|N| - |S| - 1)!}{|N|!} [f(S\cup\{i\}) - f(S)] \tag{9}$$

2.3. Genetic algorithm

Genetic algorithms, inspired by biological evolution and grounded in Darwinian natural selection, provide a method for optimization through iterative refinement of genes, which in this context represent data

Table 2
Training conditions for selecting optimal architecture to predict heat transfer performance of the heat pipe.

Architectures	Optimizer	Learning rate	Loss function	Batch size	Epoch at best performance	Hardware	# of Parameters
ANN	Adam	0.001	Mean square error	64	995	GPU: Tesla-k80	9217
DNN					902		534,529
CNN					879		32,561
CNN with skip connection					519		40,241

points. The initial data set, represented in a binary format, is generated at random. It undergoes a fitness evaluation, and the calculation method for this fitness is critical since it influences the accuracy of the optimized outcome. In the present study, thermal resistance was chosen as the criterion for fitness assessment. Leveraging a deep learning model optimized for thermal resistance prediction, each variable was further refined. Genes exhibiting lower thermal resistance were prioritized for passing on to subsequent generations, enhancing the possibility of reaching optimized solutions. To maintain genetic diversity and avoid stagnation, mutations were introduced at a low rate in the offspring genes. These new genes replace the existing ones, and the process is iterated to yield the specified variables that minimize thermal resistance. In practical applications, optimization within a specified range is often essential. Therefore, the generation was conducted to provide optimal values within a predefined range [31]. In detail, an initial population of 1000 individuals is generated within a specified range. The thermal resistance prediction was conducted based on deep learning. In this study, the specified criterion was satisfying whether 80% of the population is maintained with the same for 100 iterations. Until satisfying the specified criteria, including the 99th iteration, new offspring are created based on the data with the lowest thermal resistance. During the mutation process, 10% of the data is randomly generated within a specified range to prevent convergence to the local minimum. The flowchart of deep learning based genetic algorithm is shown in Fig. 3. The range for optimization performance evaluation is summarized in Table 3. For assessing the optimization performance for operating conditions, both single-variable and multi-variable optimization were considered. The influence of individual variables should be evaluated to evaluate the optimization performance while understanding the combined effects of multiple variables. Optimization performance for a single variable is utilized to assess the impact of each variable. On the other hand, multi-variable optimization is employed to evaluate the combined effects of multiple variables. This approach enhances the interpretability of the optimization process as well as ensures a more comprehensive exploration of the solution. The optimization

Table 3
The range for optimization performance evaluation in accordance with parameters.

Single variable optimization	
Parameter	Range for optimization
Heat load (W)	300–600
Inclination angle (°)	0–90
Filling ratio (g)	7–36
Multi-variable optimization	
Parameter	Range for optimization
Heat load (W)	400–600
Inclination angle (°)	20–60

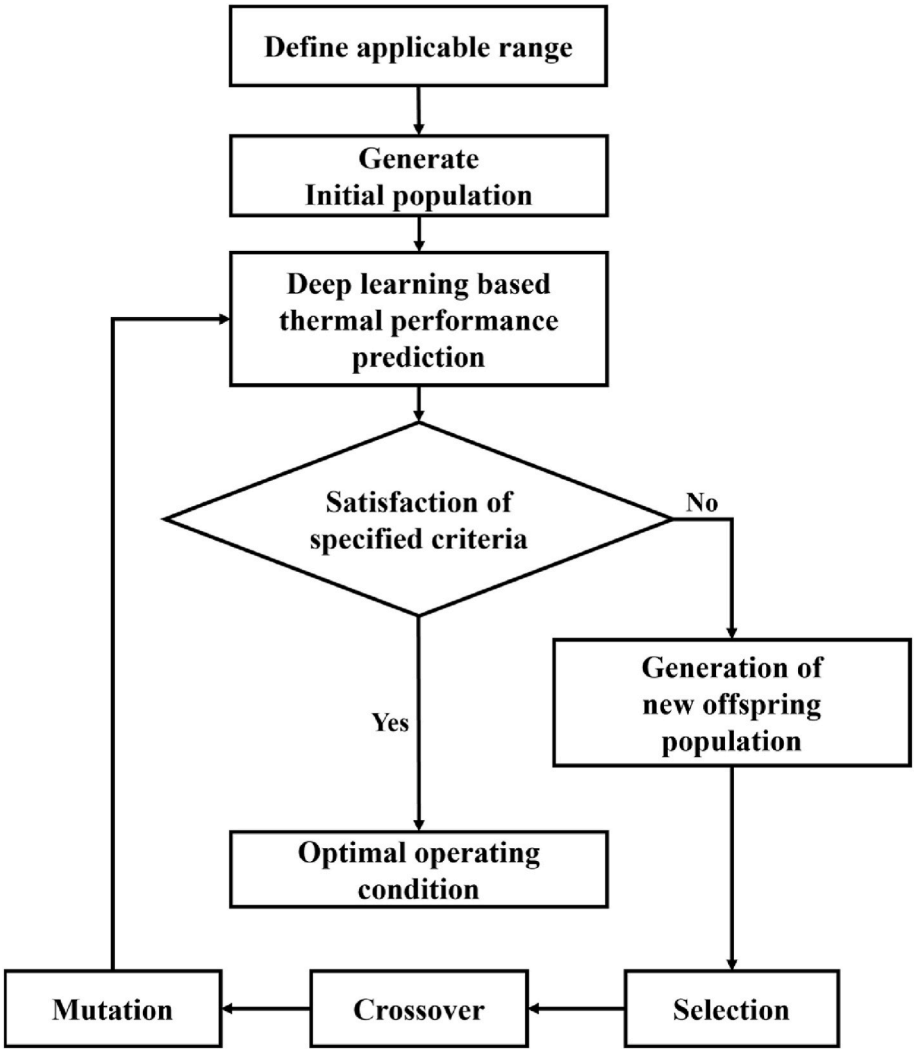

Fig. 3. Flow chart of deep learning based genetic algorithm.

strategy gains the capability to capture intricate relationships and dependencies, facilitating a more effective and informed process by evaluating single and multiple variables optimization performance. Parameters such as heat load, inclination angle, and filling ratio were evaluated for single-variable optimization, while heat load and inclination angle were considered for multi-variable cases. The optimization performance was evaluated against experimental data from published studies, confirming the utility of genetic algorithms for this type of thermal optimization.

2.4. Experimental facility

The generalization performance of a model is crucial for its applicability to unseen data. Overfitting is a common concern in machine

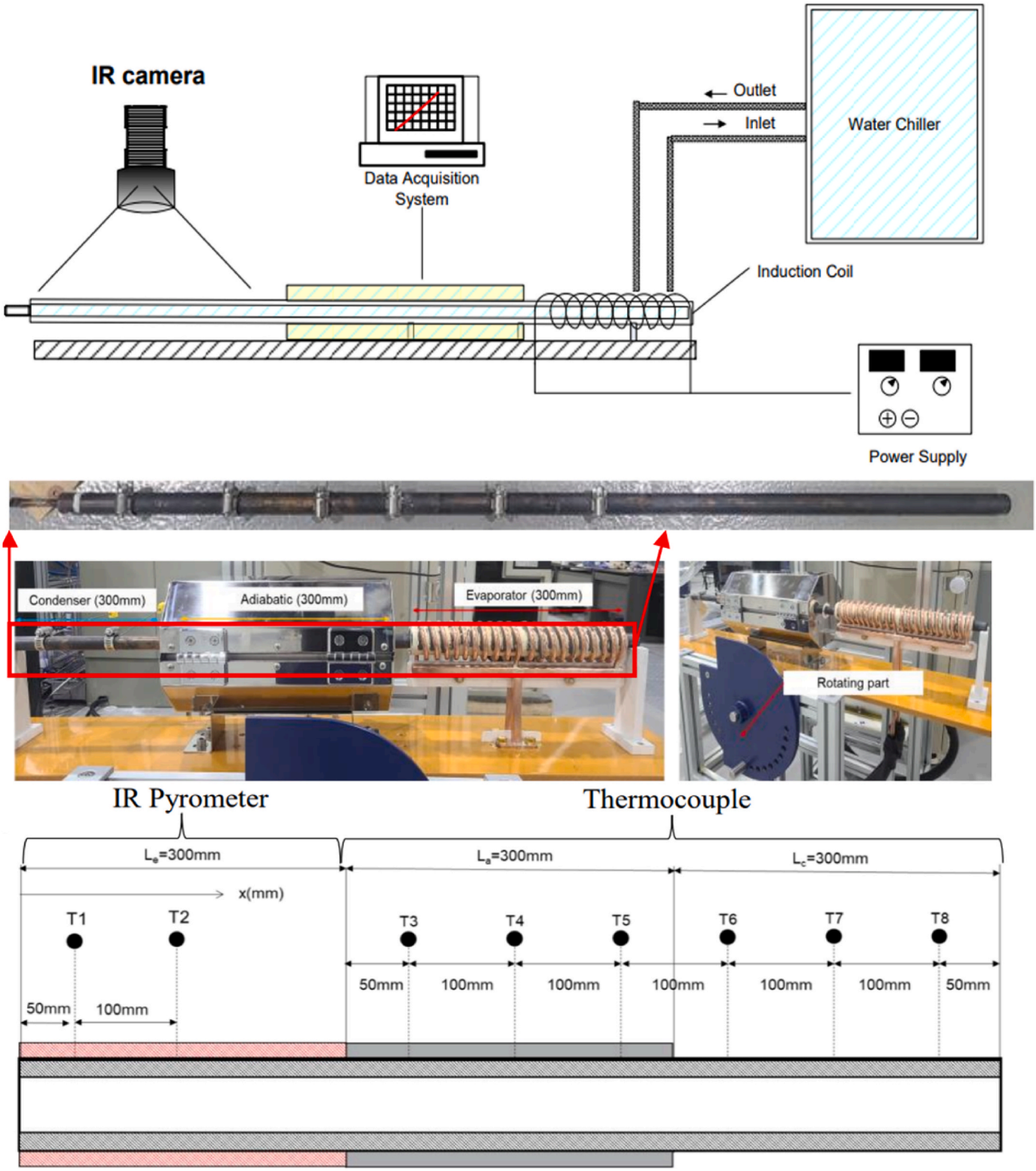

Fig. 4. Schematic illustration of test facility with TC locations [42].

learning and optimization algorithms, where a model performs well on the training data but deficiently on unseen data. In this study, additional steps were taken to mitigate the risk of overfitting and to validate the model's generalization capability. The experimental validation dataset was used to test the performance of the deep learning and genetic algorithm models. This dataset was distinct from the training dataset, allowing for a more robust assessment of the model's generalization capabilities. This is a critical aspect that often involves conditions or scenarios not explicitly covered in the training data. Thus, this study offers a more reliable and generalizable model for predicting optimal operating conditions in liquid metal heat pipes. This level of validation is critical for the practical application of these predictive models and optimization algorithms, especially in high-temperature industries where the concerns are high for both performance and safety.

The layout of the test facility is detailed in Fig. 4, incorporating elements that include an Radio-Frequency (RF) induction heat source, a thermally insulated furnace, infrared thermal measurement devices, and K-thermocouples (TCs), along with an infrared imaging system. RF-based induction heating was chosen due to its capacity to facilitate elevated temperatures within the heat pipe, thereby allowing the study of diverse thermal boundary conditions, including rapid thermal transfer and instantaneous power cut-off. The copper coil used in the induction mechanism has dimensions of 32 mm in diameter and a length of 300 mm. To maintain thermal equilibrium, a water circulation system was integrated within the coil. The induction heating unit has a maximum power output of 40 kW at a standard frequency of 50 kHz, with controllable current intensity ranging from 10 to 100 A. The initial current setting was at 10 A and was incremented in steps of 5 A. Measuring 900 mm in length and with an outer diameter of 19.05 mm, the sodium-filled pipe was designed to ensure sufficient capillary action via the inclusion of 12 layers of a #120 mesh. Contrary to the literature used for the database, the filling ratio was 260% of the wick volume with sodium. Furthermore, the length ratio of the condensation section was adjusted to consider out range of the training dataset. A comprehensive overview of the sodium heat pipe specifications is summarized in Table 4.

The heat pipe was cooled by natural air cooling. To understand the energy dynamics of heat input, loss, and cooling during the tests, we assessed the energy distribution in each section using the formulas provided in Equations. (10) – (13).

$$\dot{Q}_{RF} = \dot{Q}_{RF,Heat\ input} - \dot{Q}_{RF,cooling} \tag{10}$$

$$\dot{Q}_{loss} = \dot{Q}_{e,conv} + \dot{Q}_{e,radiation} + \dot{Q}_{a,convection} \tag{11}$$

$$\dot{Q}_{Total\ loss} = \dot{Q}_{loss} + \dot{Q}_{RF,cooling} \tag{12}$$

$$\dot{Q}_{HP,cooling} = \dot{Q}_{a,radiation} + \dot{Q}_{c,conv} + \dot{Q}_{c,radiation} \tag{13}$$

Utilizing the recorded wall temperatures as representative data points, both convective and thermal radiation heat transfers in individual segments were determined through the formulas in Equations. (14) – (17). This estimates the cumulative cooling effectiveness and rate of heat loss. The heat transfer coefficient (h_c) was deduced using the Churchill and Chu correlation for natural convection, while the emissivity (ε) of the heat pipe's surface was ascertained by calibrating temperature readings from the thermocouple and IR camera. At a steady state, the power discrepancy between RF input and total heat loss stayed below 10%.

Table 4
Configuration of sodium heat pipe.

Parameter	Range	
	Case 1	Case 2
Removed Heat (W)	400–750	200–650
Inclination angle (°)	0	
Filling ratio (g)	59.4 (260%)	
Inner diameter (mm)	19.05	
Outer diameter (mm)	16.57	
Le/L (%)	33.33	
La/L (%)	33.33	33.33
Lc/L (%)	33.33	66.67
L (mm)	900	
Working fluid	99.7% pure sodium	
Wick porosity	0.634 (120#)	
Wick thickness (mm)	1.12	

Table 5
Uncertainty of measurement instruments.

Parameter	Instruments	Uncertainties
Temperature (T)	Thermocouple (K-type)	0.75%
	Pyrometer	0.5%
Water flow rate	Turbine flowmeter	0.05%
Voltage (V)	Voltmeter	1.0%
Current (I)	Amperometry	1.0%

$$\dot{Q}_{RF,Heat\ Input} = IV \tag{14}$$

$$\dot{Q}_{RF,cooling} = \dot{m}C_p(T_{inlet} - T_{outlet}) \tag{15}$$

$$\dot{Q}_{conv} = \sum_{i=1}^{n} \pi D_o(x_{i+1} - x_i)h_c(T_i - T_\infty) \tag{16}$$

$$\dot{Q}_{rad} = \sum_{i=1}^{n} \sigma\varepsilon\pi D_o(x_{i+1} - x_i)\left(T_i^2 + T_\infty{}^2\right)(T_i + T_\infty) \tag{17}$$

The overall thermal resistance was calculated from the temperature distribution of the evaporation and condensation sections based on Equation (18), where $\overline{T}_e$ is the average temperature in evaporator section, $\overline{T}_c$ is the average temperature in condenser section, and Q_e is amount of cooling.

$$R = \frac{\overline{T}_e - \overline{T}_c}{Q_e} \tag{18}$$

2.4.1. Uncertainty analysis

The uncertainty analysis for each heat transfer parameter was performed based on the uncertainties of the measurement instruments. The uncertainty analysis for each heat transfer parameter was performed based on Equations (19)–(25). The uncertainties for each measurement instrument are listed in Table 5.

$$\frac{\partial Q_{RF,Heat\ Input}}{Q_{RF,Heat\ Input}} = \sqrt{\left(\frac{I\partial V}{Q_{RF,Heat\ Input}}\right)^2 + \left(\frac{V\partial I}{Q_{RF,Heat\ Input}}\right)^2} = \pm 1.41 \sim 1.44\% \tag{19}$$

$$\frac{\partial Q_{RF,cooling}}{Q_{RF,cooling}} = \frac{1}{Q_{RF,cooling}}\sqrt{\left(C_p\Delta T\partial\dot{m}\right)^2 + \left(\dot{m}C_p\partial\Delta T\right)^2} = \sqrt{\left(\frac{\partial\dot{m}}{\dot{m}}\right)^2 + \left(\frac{\partial\Delta T}{\Delta T}\right)^2} = \pm 0.90 \sim \pm 6.60\% \tag{20}$$

$$\frac{\partial Q_{RF}}{Q_{RF}}=\frac{1}{Q_{RF}}\sqrt{\left(\partial Q_{RF,Heat\ Input}\right)^2+\left(\partial Q_{RF,Cooling}\right)^2}=\pm 4.08\sim\pm 12.99\% \quad (21)$$

$$\frac{\partial Q_{rad}}{Q_{rad}}=\sqrt{\left(\frac{\partial D}{D}\right)^2+\left(\frac{\partial x}{x}\right)^2+\left(\frac{\partial \varepsilon}{\varepsilon}\right)^2+\left(\frac{\partial\left(T_i^2+T_\infty^2\right)}{T_i^2+T_\infty^2}\right)^2+\left(\frac{\partial\left(T_i+T_\infty\right)}{T_i+T_\infty}\right)^2}=\pm 1.22\% \quad (22)$$

$$\frac{\partial Q_{conv}}{Q_{conv}}=\sqrt{\left(\frac{\partial D}{D}\right)^2+\left(\frac{\partial x}{x}\right)^2+\left(\frac{\partial h_c}{h_c}\right)^2+\left(\frac{\partial \Delta T}{\Delta T}\right)^2}=\pm 1.58\% \quad (23)$$

$$\frac{\partial Q_{HP,Cooling}}{Q_{HP,Cooling}}=\frac{1}{Q_{HP,Cooling}}\sqrt{\left(\partial Q_{rad,a}\right)^2+\left(\partial Q_{conv,c}\right)^2+\left(\partial Q_{rad,c}\right)^2}=\pm 4.05\sim 4.89\% \quad (24)$$

$$\frac{\partial R}{R}=\frac{1}{R}\sqrt{\left(\partial Q_{HP,cooling}\right)^2+\left(\partial \overline{T}_e\right)^2+\left(\partial \overline{T}_c\right)^2} \quad (25)$$

The RF heating input's maximum uncertainty was 1.44%. The maximum uncertainty related to RF cooling was 6.60%. By incorporating the uncertainty in surface temperature to the assessment of heat transfer rate, the resulting maximum uncertainty for natural convection was found to be 1.58% and for radiation, it was 1.22%. Consequently, the total uncertainty in the heat transfer rate for the sodium heat pipe was determined to be 4.89%. The maximum uncertainty observed for thermal resistance was 9.08%. There are two reasons for the maximum uncertainty of thermal resistance. The maximum uncertainties are observed due to the effect of overfilling. For another reason, in case 2 of the experiment, the length of the condensation section was set excessively to simulate various conditions, which made fully-activated condition difficult. The maximum uncertainty of thermal resistance was confirmed under low heat load conditions, which was induced by the increased temperature difference between the condensation section and the evaporation section. Because the thermal resistance of the heat pipe is near or below 1, a 9% error corresponds to approximately 0.1, which is numerically insignificant. Therefore, uncertainty analysis is deemed to ensure rationality and reliability.

3. Results and discussion

The assessment of prediction performance for heat transfer in the liquid metal heat pipe was carried out using both the validation and test datasets. Upon identifying the optimal architecture by examining the prediction performance of ANN, DNN, and CNN, the optimal deep learning architecture was integrated into the genetic algorithm. Subsequent to evaluating the performance of the genetic algorithm, the performance of generalization was investigated by the experimental data, which is not included in the training range.

3.1. Selection of optimal deep learning architecture

The predictive performance of ANN, DNN, CNN, and CNN with skip connections were analyzed to discover the optimal architecture for heat pipe heat transfer when using liquid metal as the working fluid. Fig. 5 shows the PE relative to the reference thermal resistance with detail metrics such as MAE, MSE, MAPE, and the coefficient of determination for each architecture. The ANN architecture for the prediction of thermal performance showed inadequate prediction performance, characterized by the highest maximum percentage error. The predictive performance of the DNN model was similar to the basic CNN architecture. However, the CNN architecture had a diminished maximum percentage error compared to the DNN model. Therefore, this study tried to enhance the CNN model's prediction performance by incorporating the skip connections method. Both the comprehensive performance and the maximum percentage error of the CNN architecture with skip connections surpassed that of the basic CNN model for predicting liquid metal heat pipe thermal performance. The fundamental difference in performance between the basic ANN structure and CNN is attributed to the number of parameters. Typically, as the number of parameters increases, the performance of deep learning models tends to improve. However, the maximum PE of DNN was high compared to CNN. The process of CNN to handle the spatial structure of data is considered the reason for performance enhancement, despite having a larger number of parameters of DNN. CNNs, equipped with convolutional layers, have shown outstanding performance in capturing specific features. While CNN can identify complex patterns crucial for accurately predicting the performance of heat pipes, ANN and DNN have the inherent difficulty of identifying such subtle relationships with a lack of certain mechanisms, leading to performance deterioration. As a result, the architecture of the CNN with skip connections was considered to be used for the genetic

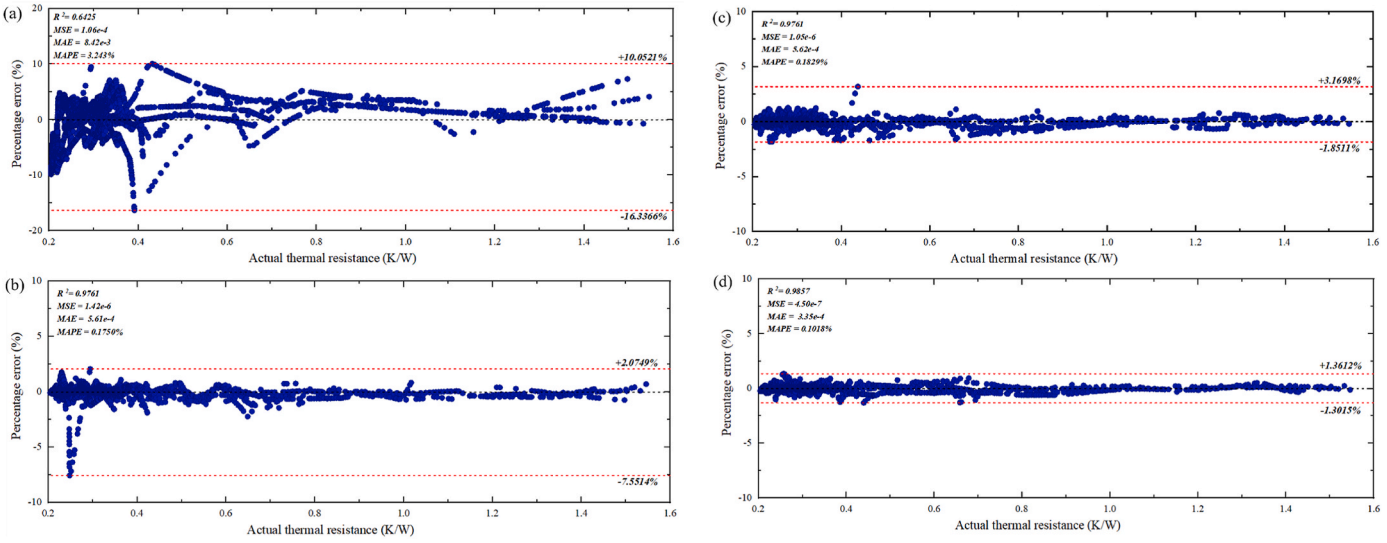

Fig. 5. The prediction performance comparison of each architecture: (a)ANN, (b) DNN, (c) CNN, and (d) CNN with skip connection.

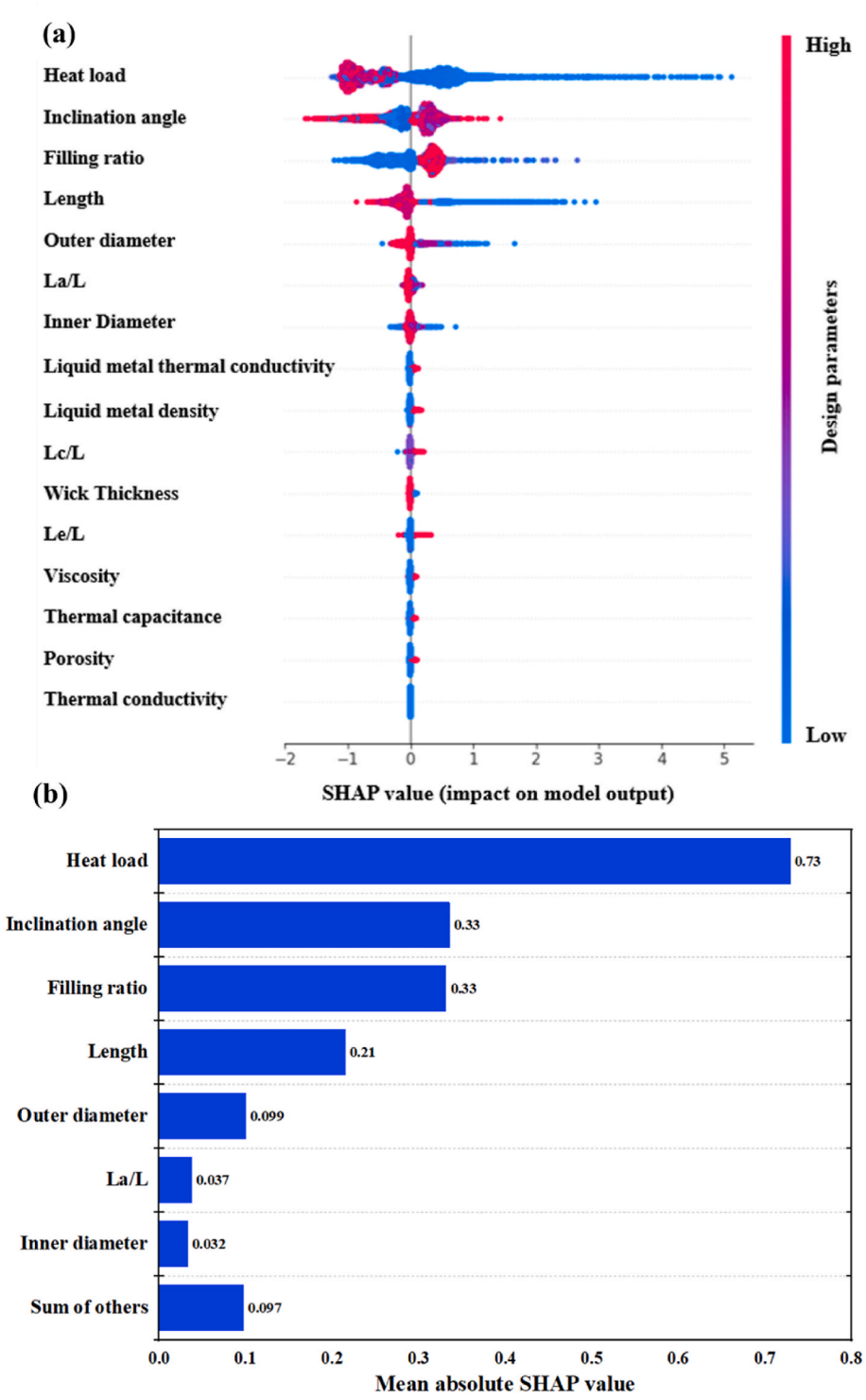

Fig. 6. Influence of design parameters for prediction performance: (a) SHAP value in accordance with the range, and (b) mean absolute SHAP value.

algorithm to predict the heat transfer performance of liquid metal heat pipes.

The SHAP analysis was applied to the CNN with skip connection architecture, which represents the outstanding prediction performance. Evaluating the impact of design parameters on deep learning architecture with reliable prediction performance could offer valuable design guidelines. Fig. 6 illustrates the influence of each design parameter, arranged in order of descending significance. Fig. 6 (a) depicts the influence on predictions according to design parameters. Fig. 6 (b) represents the mean absolute SHAP values for design parameters. In terms of heat pipe heat transfer performance, the most influential design parameter was the heat load, followed by the inclination angle and filling ratio. Increasing the heat load is considered crucial for enhancing the heat transfer performance of heat pipes. The inclination angle and filling ratio depend on other conditions. For length and outer diameter, providing sufficient length is considered essential for increasing heat transfer performance. The optimization performance evaluation was conducted for the three most influential design parameters.

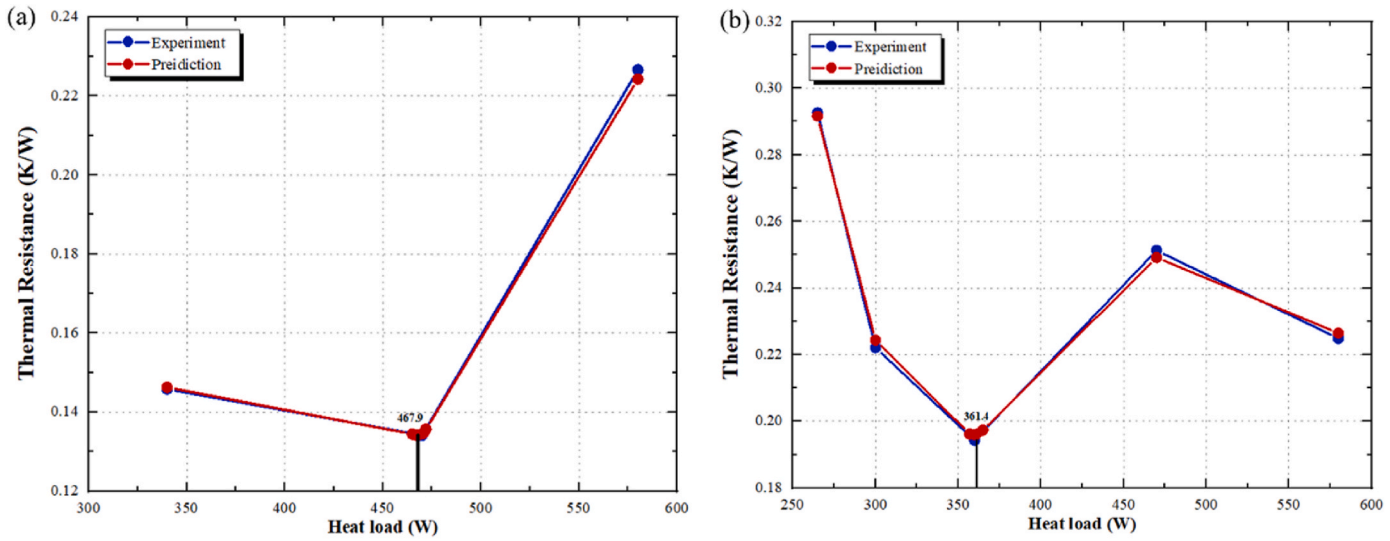

Fig. 7. The comparison of optimization performance with experimental result for heat load: (a) 60° and (b) 75°

Table 6
Optimization performance for a Heat load.

Inclination (°)	Experiment (W)	Optimization (W)	Error (%)
30	470	469.7	0.064
60	470	467.9	0.447
75	360	361.4	0.389

Table 7
Optimization performance for a inclination angle.

Heat load(W)	Experiment (°)	Optimization (°)	Error (%)
370	15	13.5	10
400	0	0	0
550	0	0	0
2500	15	12.3	18

3.2. Single variable optimization performance

3.2.1. Heat load

The performance of optimization was evaluated by comparing the percentage error for each variable against experimental data obtained from experimental investigation literature. The data range for optimizing operating conditions was determined from the bounds of the experimental findings. For heat load of optimal operation condition, a heat pipe of 800 mm in length, filled with 20g and using potassium as the working fluid, was assessed at inclination angles of 30°, 60° and 75°. Fig. 7 and Table 6 illustrates the comparative optimization outcomes for heat load against experimental data. The results for optimizing the heat load were exceptional, proving less than a 1% maximum PE. A contributing factor to this superior performance in heat load optimization compared to other parameters could be the data augmentation, which was primarily centered around the heat load.

3.2.2. Inclination angle

For the operating condition optimization of the inclination angle, a heat pipe with an 800 mm length, filled with 20g and 100g, and utilizing potassium as its working fluid, was evaluated under heat loads of 370 W, 400 W, 550 W, and 2500 W. Both Fig. 8 and Table 7 illustrate the results of the inclination angle optimization in comparison to the observed empirical values. The results showed that the optimization performance pertaining to the inclination angle remains inferior. While the

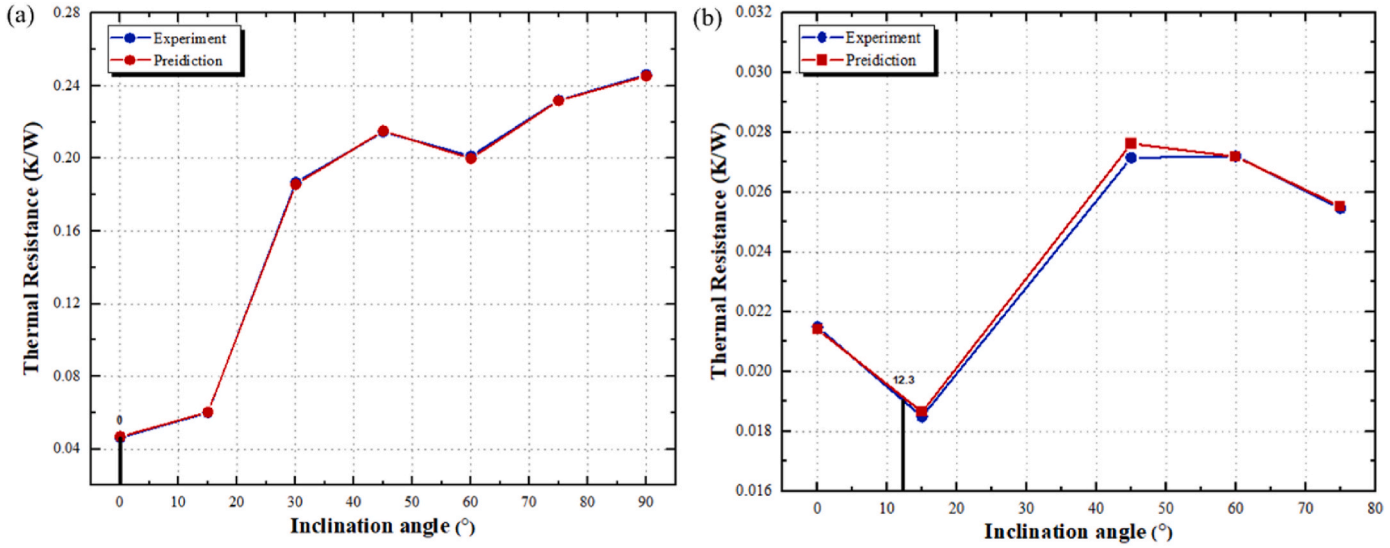

Fig. 8. The comparison of optimization performance with experimental result for inclination angle: (a) 400 W and (b) 2500 W.

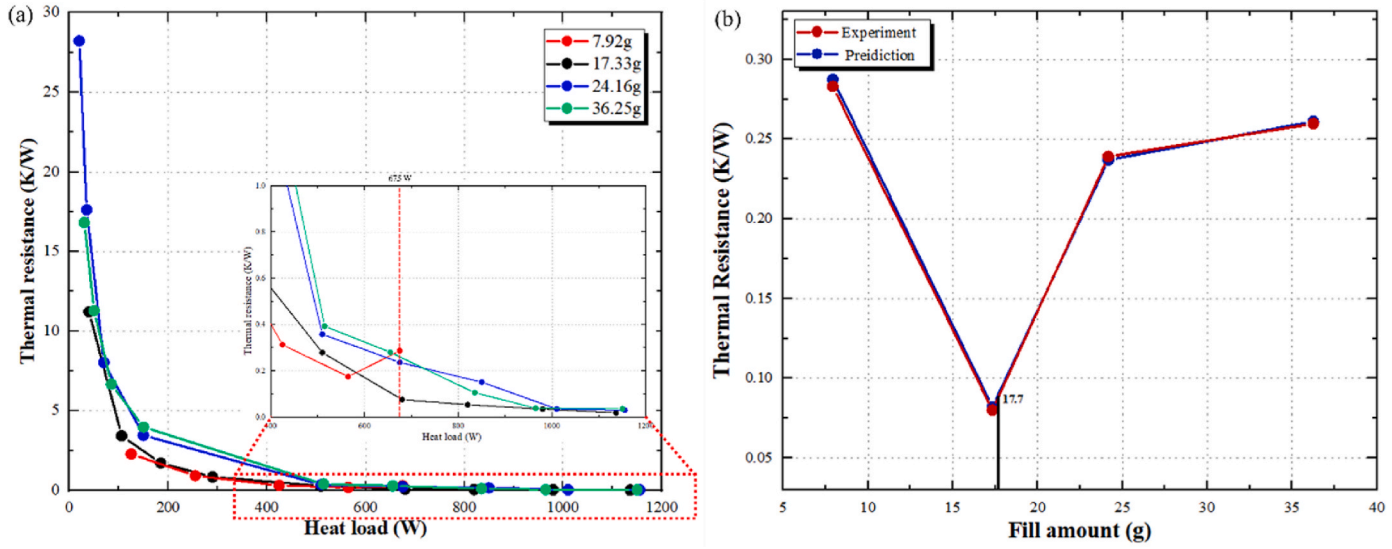

Fig. 9. Comparison of optimization performance for Filling ratio: (a) experimental data (b) optimization result.

discrepancy between the empirical data and the optimized data is merely 2.7°, the peak PE reached up to 18%. It is considered that the performance inconsistency in inclination angle optimization arises because the magnitude of the inclination angle is relatively low in comparison to the heat load. It is regarded that the optimization and prediction model proceed sensitively to variations in the inclination angle.

3.2.3. *Filling ratio*

For the optimization of the filling ratio, a heat pipe with a length of 350 mm and sodium as its working medium was examined under a 675 W heat load. Fig. 9 illustrates the performance of filling ratio optimization, including comparison to experimental investigation. The performance of the filling ratio optimization was a low PE of 2.09%. The optimization performance for this single variable demonstrates a reasonable level. Therefore, the optimization method could be applied to be beneficial across various high-temperature applications.

Table 8
Optimization performance for multi-variables.

Parameter	Experiment	Optimization	Error (%)
Heat load (W)	470	461.8	1.75
Inclination angle (°)	20	21.5	7.5

3.3. *Multi-variable optimization performance*

The optimization performance for multiple variables, as well as single variables, was also confirmed. For the performance evaluation of multivariable optimization, the heat load and inclination angle are considered. The range of heat load was from 400 W to 500 W and the range of inclination angle was from 20° to 90° for liquid metal heat pipe thermal performance optimization. The optimization performance is shown in Fig. 10 and Table 8 with a comparison to the experimental investigation. Optimization performance was reasonable for multivariate optimization. Comparing the performance of single-variable optimization, the errors of the inclination angle and heat load was similar levels. Since the multi-variable optimization performance does not differ

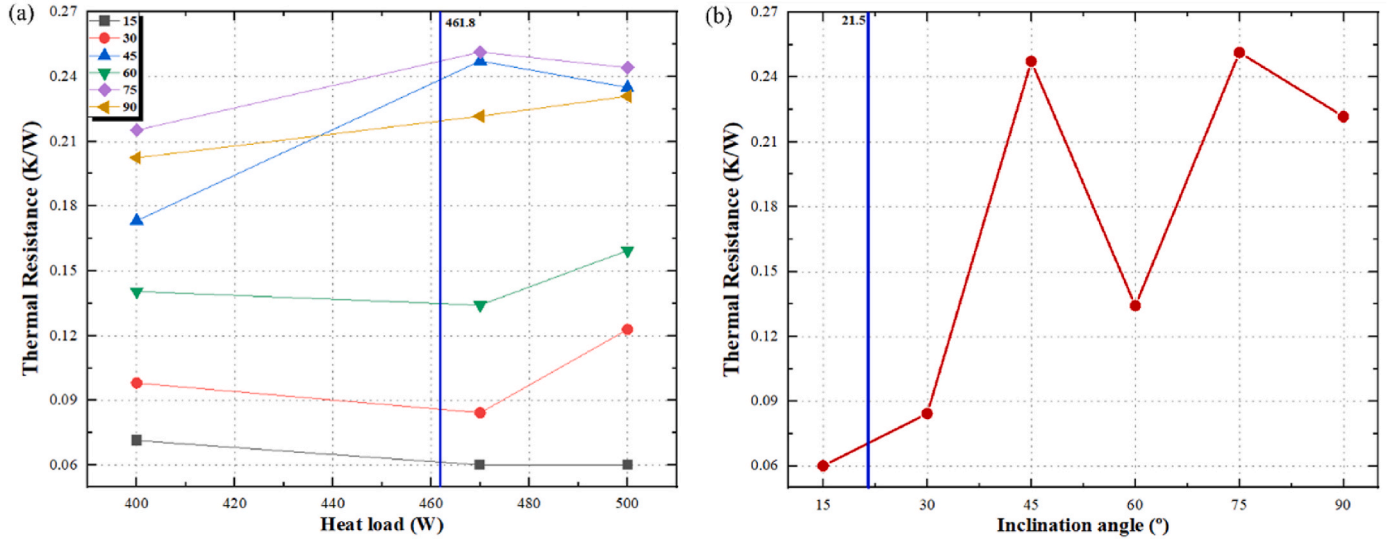

Fig. 10. Optimization performance for multi-variables with the reference dataset: (a) Heat load data (b) Inclination angle data.

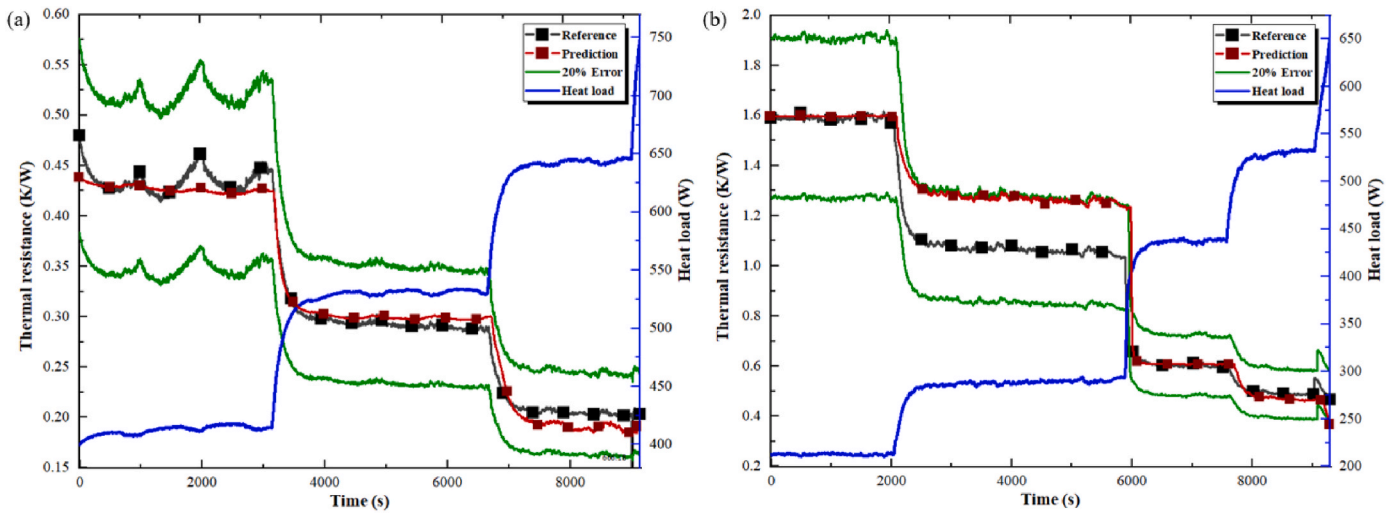

Fig. 11. Optimization performance for experimental datasets outside the range of training dataset: (a) Case 1 (b) Case 2.

Table 9
Optimization performance for experimental validation dataset.

Type	Experiment (W)	Optimization (W)	Error (%)
Case 1	666.18	680.7	2.18
Case 2	668.67	665.5	0.47

significantly from the single-variable optimization performance, the optimization performance would be guaranteed even if a variable is added.

3.4. Generalization performance

To evaluate the generalization performance of the optimization model, a comparison was conducted with experimental data outside the range of the training data. Heat load was selected as a variable for optimization. The behavior of the prediction model and optimization performance are shown in Fig. 11 and Table 9. In Case 1 and Case 2, the experimental and predicted values of thermal resistance according to heat load were compared, and the goal was to find the optimal heat load by using a deep learning model and genetic algorithm. The thermal resistance behavior according to the heat load change of the liquid metal heat pipe was reasonably predicted, and the error was low for the optimal value. However, the prediction performance was lower than the previous, which is considered to be due to the difference between the overfilled liquid metal heat pipe and the general liquid metal heat pipe. Nevertheless, the predicted thermal resistance followed well the thermal resistance behavior of the overfilled liquid metal heat pipe, which was not included in the training dataset. In conducting transient numerical analysis of liquid metal heat pipes, performance was demonstrated with a maximum deviation ranging between 16% and 23%, depending on the considered scenarios [43,44]. In this study, a deep learning model predicts the thermal resistance within a 20% error in transient conditions. Therefore, the prediction performance of the deep learning model is considered reasonable. Although the prediction performance of the deep learning model is similar to that of previous numerical analysis models, it has an advantage in utilizing thermal properties before the operation

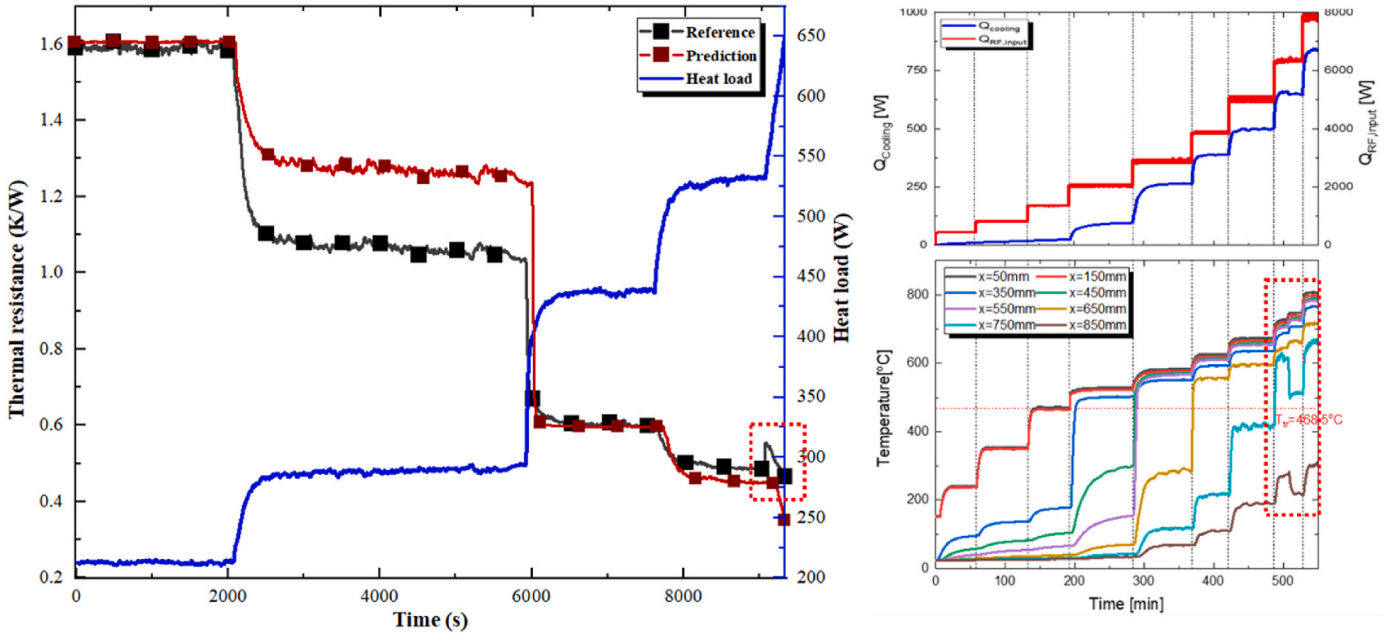

Fig. 12. Behavior of temperature and thermal resistance of the sodium heat pipe for case 2.

of the heat pipe compared to the numerical analysis method. Numerical analysis methods require thermal properties, which are obtained from the experiment, under specific conditions for accurate predictions. Furthermore, the thermal resistance was predicted within 1 s. The deep learning model could contribute to saving costs and time in the absence of experimental validation. In case of the optimization, offering conditions for the lowest thermal resistance is important by following the behavior. Therefore, the difference with the predicted value is not considered to be a significant problem.

In particular, when predicting the heat transfer performance of the liquid metal heat pipe, the influence of the sudden temperature decreases in the cooling part that occurred in case 2 could not be predicted. The overall temperature, thermal resistance, and heat load behavior of the sodium heat pipe for case 2 are shown in Fig. 12. The reason is considered due to the operation difference between the overfilled liquid metal heat pipe and the general liquid metal heat pipe since the data of the general liquid metal heat pipe is used for training. When deep learning was trained, it could not reflect the characteristics of the heat pipe with a filling amount of 260% of the wick volume because such a heat pipe wasn't taken into account. It is considered that a database should consider heat pipes with various characteristics, and further experimental investigations related to the heat transfer of liquid metal heat pipes are necessary for various operational conditions. Nevertheless, the generalization performance of the optimization model was found to be outstanding. This optimization method can contribute to reducing manufacturing time and cost by offering an optimal liquid metal heat pipe before application to a micro-reactor or various nuclear reactors. Furthermore, could be applied to the heat pipe application for high-temperature fields.

4. Conclusion

Heat pipes, especially those using liquid metal as the working fluid, have gathered significant attention due to their efficient heat transfer capabilities. These heat pipes are essential components in high-temperature applications, including microreactors, various nuclear reactors, and other high-temperature fields. Therefore, optimizing operating conditions could result in reduced manufacturing time and decreased costs. In this study, an optimization approach using deep learning models and genetic algorithms was suggested to resolve the intricate dynamics of heat transfer within liquid metal heat pipes. The performance assessment was conducted for single-variable optimization of operating conditions such as heat load, inclination angle, and filling ratio, and extended to multi-variable optimization. The results proved reasonable performance, with the optimization process yielding a low percentage of errors in most cases with 18% of the maximum PE. However, a crucial aspect of any predictive model is its ability to generalize to unseen data. The generalization performance was evaluated using datasets that were outside its training range. While the model exhibited reasonable prediction performance, some shortcomings were identified, particularly when dealing with overfilled liquid metal heat pipes. This highlighted the importance of diverse and representative training datasets. The need for this research stems from the evolving landscape of high-temperature applications and the critical role of heat pipes within them. As the demand for efficient heat transfer solutions grows, so does the necessity for optimizing these systems. In conclusion, this study underscores the potential of system optimization, in predicting and optimizing heat transfer in liquid metal heat pipes. However, when assessing the model's generalization capabilities using data outside the training range, certain challenges emerged, particularly with overfilled heat pipes. Furthermore, this study could not reflect other wick types due to the limitation of literature. These limitations emphasized the need for a more diverse training database. Hence, for improved applicability, this study encourages the experimental investigation for various operating conditions. Even with these challenges, the overall outlook of the study is positive. The optimization methodology developed herein could revolutionize the design and application of heat pipes in various high-temperature industries, emphasizing the pressing need for such research endeavors.

Declaration of interest Statement

The authors declare that they have no known competing financial interests or personal relationships that could have appeared to influence the work reported in this paper.

Acknowledgments

This work was supported by the National Research Foundation of Korea (NRF) grant funded by the Korean government (MSIT) (no. 2021M2D2A1A03048950).

References

[1] K.M. Kim, Y.S. Jeong, I.C. Bang, Thermal analysis of lithium ion battery-equipped smartphone explosions, Engineering Science and Technology, an International Journal 22 (2) (2019) 610–617.
[2] X. Tang, Z. Quan, Y. Zhao, Experimental investigation of solar panel cooling by a novel micro heat pipe array, Energy Power Eng. 2 (3) (2010) 171–174.
[3] K.M. Kim, I.C. Bang, Heat transfer characteristics and operation limit of pressurized hybrid heat pipe for small modular reactors, Appl. Therm. Eng. 112 (2017) 560–571.
[4] I.G. Kim, I.C. Bang, Spent nuclear fuel with a hybrid heat pipe for electricity generation and thermal management, Energy Convers. Manag. 173 (2018) 233–243.
[5] C. Wang, J. Chen, S. Qiu, W. Tian, D. Zhang, G.H. Su, Performance analysis of heat pipe radiator unit for space nuclear power reactor, Ann. Nucl. Energy 103 (2017) 74–84.
[6] J.Y. Kim, Y.Y. Park, I.C. Bang, Performance analysis of heat pipe-based passive in-core decay heat removal system for the small modular reactor design with MARS-KS code, Ann. Nucl. Energy 194 (2023) 110091.
[7] K.M. Kim, Y.S. Jeong, I.G. Kim, I.C. Bang, Development of passive in-core cooling system for nuclear safety using hybrid heat pipe, Nucl. Technol. 196 (3) (2016) 598–613.
[8] D.I. Poston, The heatpipe-operated Mars exploration reactor (HOMER), AIP Conf. Proc. 552 (No. 1) (2001, February) 797–804. American Institute of Physics.
[9] M.S. El-Genk, J.M.P. Tournier, "SAIRS"—scalable Amtec integrated reactor space power system, Prog. Nucl. Energy 45 (1) (2004) 25–69.
[10] M.S. El-Genk, J.M. Tournier, Performance analysis of potassium heat pipes radiator for HP-STMCs space reactor power system, AIP Conf. Proc. 699 (No. 1) (2004, February) 793–805. American Institute of Physics.
[11] A. Bushman, D.M. Carpenter, T.S. Ellis, S.P. Gallagher, M.C. Hershcovitch, M. C. Hine, M.A. Stawicki, The Martian Surface Reactor: an Advanced Nuclear Power Station for Manned Extraterrestrial Exploration, MIT-NSA-TR-003, 2004.
[12] D. Palac, M. Gibson, L. Mason, M. Houts, P. McClure, R. Robinson, Nuclear Systems Kilopower Overview (No. GRC-E-DAA-TN29740), 2016.
[13] P.R. Mcclure, D.I. Poston, V.R. Dasari, R.S. Reid, Design of Megawatt Power Level Heat Pipe Reactors, Report of Los Alamos National Laboratory, USA, 2015.
[14] A. Levinsky, J.J. van Wyk, Y. Arafat, M.C. Smith, Westinghouse eVinci reactor for off-grid markets, Transactions 119 (1) (2018) 931–934.
[15] H. Yang, C. Wang, D. Zhang, J. Zhang, W. Tian, S. Qiu, G.H. Su, Parameter sensitivity study on startup characteristics of high temperature potassium heat pipe, Nucl. Eng. Des. 392 (2022) 111754.
[16] H. Sun, X. Liu, H. Liao, C. Wang, J. Zhang, W. Tian, S. Qiu, G. Su, Experiment study on thermal behavior of a horizontal high-temperature heat pipe under motion conditions, Ann. Nucl. Energy 165 (2022) 108760.
[17] Z. Tian, J. Zhang, C. Wang, K. Guo, Y. Liu, D. Zhang, W. Tian, S. Qiu, G.H. Su, Experimental evaluation on heat transfer limits of sodium heat pipe with screen mesh for nuclear reactor system, Appl. Therm. Eng. 209 (2022) 118296.
[18] L.H. Cisterna, M.C. Cardoso, E.L. Fronza, F.H. Milanez, M.B. Mantelli, Operation regimes and heat transfer coefficients in sodium two-phase thermosyphons, Int. J. Heat Mass Transf. 152 (2020) 119555.
[19] C. Wang, L. Zhang, X. Liu, S. Tang, S. Qiu, G.H. Su, Experimental study on startup performance of high temperature potassium heat pipe at different inclination angles and input powers for nuclear reactor application, Ann. Nucl. Energy 136 (2020) 107051.
[20] Z. Tian, X. Liu, C. Wang, D. Zhang, W. Tian, S. Qiu, G.H. Su, Experimental investigation on the heat transfer performance of high-temperature potassium heat pipe for nuclear reactor, Nucl. Eng. Des. 378 (2021) 111182.
[21] C. Wang, X. Liu, M. Liu, S. Tang, Z. Tian, D. Zhang, W. Tian, S. Qiu, G. Su, Experimental study on heat transfer limit of high temperature potassium heat pipe for advanced reactors, Ann. Nucl. Energy 151 (2021) 107935.
[22] Y. Ma, H. Yu, S. Huang, Y. Zhang, Y. Liu, C. Wang, R. Zhong, X. Chai, C. Zhu, X. Wang, Effect of inclination angle on the startup of a frozen sodium heat pipe, Appl. Therm. Eng. 201 (2022) 117625.

[23] R. Manoj, M. Kumar, R. Narasimha Rao, K. Rama Narasimha, P.V.S. Suresh, Performance evaluation of sodium heat pipe through parameteric studies, Frontiers in Heat Pipes (FHP) 3 (4) (2013).
[24] A.A. El-Nasr, S.M. El-Haggar, Effective thermal conductivity of heat pipes, Heat Mass Tran. 32 (1–2) (1996) 97–101.
[25] S. Mahjoub, A. Mahtabroshan, Numerical Simulation of a conventional heat pipe, World Academy of Science, Engineering and Technology 39 (2008) 117–122.
[26] Z. Tian, C. Wang, J. Huang, K. Guo, D. Zhang, X. Liu, G.H. Su, W. Tian, S. Qiu, Code development and analysis on the operation of liquid metal high temperature heat pipes under full condition, Ann. Nucl. Energy 160 (2021) 108396.
[27] T. Kaya, J. Goldak, Numerical analysis of heat and mass transfer in the capillary structure of a loop heat pipe, Int. J. Heat Mass Tran. 49 (17–18) (2006) 3211–3220.
[28] A.B. Solomon, M. Sekar, S.H. Yang, Analytical expression for thermal conductivity of heat pipe, Appl. Therm. Eng. 100 (2016) 462–467.
[29] C. Wang, Z. Zhang, M. Zhang, P. Li, Z. Tian, W. Tian, S. Qiu, G.H. Su, Numerical evaluation of non-condensable gas influence on the heat transfer characteristics of high-temperature lithium heat pipe during reactor operation, Ann. Nucl. Energy 173 (2022) 109077.
[30] I.J. Jin, Y.Y. Park, I.C. Bang, Heat transfer performance prediction for heat pipe using deep learning based on wick type, Int. J. Therm. Sci. 197 (2024) 108806.
[31] I.J. Jin, I.C. Bang, Deep learning based thermal performance optimization for the liquid metal heat pipe, in: Proceeding of International Topical Meeting on Nuclear Reactor Thermal Hydraulics (NURETH-20), Washington D.C., 2023.
[32] K. Kumararaja, C.S. Khiran Kumar, B. Sivaraman, A convolutional neural network analysis of a heat pipe with Hybrid Nanofluids, Int. J. Ambient Energy (2021) 1–13.
[33] V.M. Patel, H.B. Mehta, Thermal performance prediction models for a pulsating heat pipe using Artificial Neural Network (ANN) and Regression/Correlation Analysis (RCA), Sādhanā 43 (11) (2018) 1–16.
[34] Y. Naresh, Numerical investigation on the heat transfer performance and optimisation of a finned heat pipe using artificial neural networks and genetic algorithm, Int. J. Ambient Energy 43 (1) (2022) 2231–2238.
[35] X. Wang, B. Li, Y. Yan, N. Gao, G. Chen, Predicting of thermal resistances of closed vertical meandering pulsating heat pipe using artificial neural network model, Appl. Therm. Eng. 149 (2019) 1134–1141.
[36] C. Oh, S. Han, J. Jeong, Time-series data augmentation based on interpolation, Procedia Computer Science 175 (2020) 64–71.
[37] Q. Wen, L. Sun, F. Yang, X. Song, J. Gao, X. Wang, H. Xu, Time Series Data Augmentation for Deep Learning: A Survey, 2020 arXiv preprint arXiv: 2002.12478.
[38] H. Chen, W. Han, D. Yang, S. Poria, DoubleMix: Simple Interpolation-Based Data Augmentation for Text Classification, 2022 arXiv preprint arXiv:2209.05297.
[39] B. Yegnanarayana, Artificial Neural Networks, PHI Learning Pvt. Ltd, 2009.
[40] S. Albawi, T.A. Mohammed, S. Al-Zawi, Understanding of a convolutional neural network, in: 2017 International Conference on Engineering and Technology (ICET), Ieee, 2017, August, pp. 1–6.
[41] S.M. Lundberg, S.I. Lee, A unified approach to interpreting model predictions, Adv. Neural Inf. Process. Syst. 30 (2017).
[42] D.H. Lee, I.C. Bang, Experimental investigation of thermal behavior of overfilled sodium heat pipe, Int. J. Heat Mass Tran. 215 (2023) 124449.
[43] Z. Tian, C. Wang, J. Huang, K. Guo, D. Zhang, X. Liu, G.H. Su, W. Tian, S. Qiu, Code development and analysis on the operation of liquid metal high temperature heat pipes under full condition, Ann. Nucl. Energy 160 (2021) 108396.
[44] Z. Zhang, X. Chai, C. Wang, H. Sun, D. Zhang, W. Tian, S. Qiu, G.H. Su, Numerical investigation on startup characteristics of high temperature heat pipe for nuclear reactor, Nucl. Eng. Des. 378 (2021) 111180.